Macromolecules
ARTICLE

Macromolecules **2010**, *43*, 9747–9753 **9747**
DOI: 10.1021/ma1017082

Effect of Spin Speed and Solution Concentration on the Directed Assembly of Polymer Blends

Liang Fang, Ming Wei, Carol Barry, and Joey Mead*

NSF Nanoscale Science and Engineering Center for High-Rate Nanomanufactuing, Department of Plastics Engineering, University of Massachusetts Lowell, One University Avenue, Lowell, Massachusetts 01854, United States

Received July 29, 2010; Revised Manuscript Received October 19, 2010

ABSTRACT: Directed assembly of polymer blends using chemically heterogeneous patterns during spin-coating can be used to produce nanopatterned polymer structures. Well-ordered morphologies are obtained when the characteristic length of a polymer blend is commensurate with pattern periodicity. In this paper, spin-coating speed and solution concentration were used to control the characteristic length of a polystyrene (PS)/poly(acrylic acid) (PAA) blend. With increasing spin speed or reducing solution concentration, the characteristic length decreased. Critical spin speeds or solution concentrations that produced the required characteristic length commensurate with the given pattern periodicity were predicted. Well-ordered morphologies were obtained when spin speed or solution concentration was close to the critical value. A new method of image analysis was introduced to quantitatively evaluate the quality of replication of the underlying pattern. The range of commensurability between characteristic length and pattern periodicity for well-ordered morphologies was investigated. When the range of commensurability was within 20%, well-ordered morphologies were produced.

Introduction

Directed assembly of block copolymers and polymer blends using chemically functionalized nanopatterned templates is currently of particular interest. Patterned polymer structures with different functionalities at the nanoscale have potential applications, such as flash memory devices,[1] quantum dots,[2,3] templates for nanolithography,[4−8] and optoelectronic devices, including semiconductor transistors[9−11] and LEDs.[12−14]

The phase separation of block copolymers has been used to form highly ordered nanostructures by chemically functionalized patterned templates.[15−28] Experimental and theoretical results[5,20,22,25,26,28] demonstrated that well-ordered block copolymer morphologies were produced when the phase domain size, L, was commensurate with the pattern periodicity, λ, i.e., $L/\lambda = 1$. Nealey and co-workers[28] observed long-range order provided that the commensurability was ~10%, i.e., $0.89 < L/\lambda < 1.09$. The phase separation of polymer blends also has been used to fabricate well-ordered patterned polymer structures.[29−39] Raczkowska et al.[30] found that, similar to block copolymers, well-ordered morphologies in annealed samples were formed only when the characteristic length, R, of the unpatterned polymer blends was commensurate with the pattern periodicity, i.e., $R/\lambda = 1$. In contrast, Chiota et al.[39] directed the nanoscale assembly of polymer blends into complex patterns at multiple length scales on a single template using solvent annealing. As polymer blends are not restricted by the block length, annealing facilitates the replication of patterns with multiple length scales in a single template.

The phase-separated morphology of a polymer blend in a thin film can be described by a characteristic value of the most predominant length, e.g., characteristic length, which is usually found by fast Fourier transformation (FFT) analysis. The characteristic length of a polymer blend represents the predominant length of vectors, which are randomly drawn passing through the two phases.[40−42] The characteristic length is related to the length or size of the phase domains. It represents the repeat length from domain to domain of one of the species or the size of domains for both species. Normally, the characteristic length increases with increasing domain size. It is widely accepted that on a homogeneous substrate with a single surface energy the characteristic length of polymer blends in spin-coated films can be controlled by spin speed and solution concentration.[43−47] Walheim et al.[45] reported that the average domain size of polystyrene (PS)/poly(methyl methacrylate) (PMMA) blend decreased with increasing spin speed. Ton-That et al.[47] found that, for PS/PMMA blends, the domain size was controlled by changing solution concentration.

For the directed assembly of polymer blends on heterogeneous patterns with different functionalities, Raczkowska et al.[30] demonstrated that the characteristic length of the phase separated morphologies of PS/poly(2-vinylpyridine) (PVP) blends decreased with increasing spin speed or reducing solution concentration. The optimal replication of the pattern occurred when the characteristic length and pattern periodicity (4 μm) were commensurate. Nisato et al.[48] controlled spin speed and solution concentration to obtain well-ordered patterned morphologies of deuterated polystyrene (dPS)/polybutadiene (PB) blends on chemically functionalized patterns of 4 μm periodicity. The pattern periodicities in these studies, however, were microscale. The degree of commensuration required between the characteristic length and pattern periodicity, R/λ, on the directed assembly of polymer blends at the nanoscale has not been studied. From the manufacturing viewpoint, the control of processing conditions can significantly impact the fabrication of highly ordered polymer nanostructures and has not been fully investigated.

In this work, patterned polymer structures of PS/poly(acrylic acid) (PAA) blends were produced by directed assembly on

*Corresponding author. E-mail: joey_mead@uml.edu.

Published on Web 11/04/2010

Table 1. Spin Speeds and Solution Concentrations Used during Spin-Coating

trials	spin speed/rpm	solution concn/wt %
1−9	1000−9000	1.0
10−15	3000	0.4−1.4

chemically heterogeneous patterns, fabricated using a combination of electron beam lithography and self-assembled monolayers of alkanethiols with different functionalities.[37] Spin-coating speed and solution concentration were used to control the characteristic lengths of the phase-separated blend morphologies. Here, for the first time, the degree of the commensurability required for well-ordered assembly of polymer blends is presented.

Experimental Section

Materials. Polystyrene (PS) with weight-average molecular weight (M_w) of 18 100 Da, poly(acrylic acid) (PAA) with M_w of 2000 Da, and *N*,*N*-dimethylformamide (DMF) were purchased from Aldrich and used as received.

Assembly of PS/PAA Blends. The chemically heterogeneous patterns were produced by combining electron beam lithography and self-assembled monolayers of alkanethiols with different functionalities. This method has been described previously.[37] The nanopatterned template was placed on the rotating plate of a spin-coater. Six minutes after 70−80 μL of the polymer solution (PS/PAA with the weight ratio of 7/3 in DMF) was dropped on the template, the polymer solution was spin-coated on the template surface for 30 s. The chamber of the spin-coating machine was purged with high-purity nitrogen gas to control the humidity to less than 1%. The spin-coating speed and solution concentration were varied as shown in Table 1; trials 1−9 investigated the effects of spin speed and trials 10−15 the effects of solution concentration.

Characterization. The morphologies of PS/PAA blends were examined by field emission scanning electron microscopy (JEOL 7401F) and atomic force microscopy (PSIA, XE-150, 40 N m^{-1} tip spring constant in noncontact mode was used). To calculate the characteristic lengths of the initial morphologies of PS/PAA blends, fast Fourier transform (FFT) analyses of the corresponding atomic force microscopy (AFM) topography images were performed by AFM image analysis software XEI (PSIA Corp., Version 1.5). The FFT diagrams were used to calculate the characteristic length of the phase-separated morphologies of polymer blends.

Results and Discussion

The effects of spin speed and solution concentration on the phase-separated morphologies of PS/PAA blend on homogeneous substrates were first investigated to achieve the relationship between characteristic length and spin-coating conditions. The critical spin speeds and solution concentrations, producing the required characteristic lengths which were commensurate with the given different pattern periodicities, were predicted and verified, respectively.

Spin Speed. *Homogeneous Substrates*. To investigate the effect of spin speed on the characteristic length, the PS/PAA blend solutions were initially spin-coated at different spin speeds on homogeneous substrates with a single surface energy. Figure 1 shows the AFM topography images of the PS/PAA phase-separated morphologies on the homogeneous substrates. The bright and dark regions in the images of Figure 1 are the thick and thin areas, respectively. The bright regions corresponded to PS domains while dark areas were attributed to PAA domains.[37] The driving force for phase separation of polymer blends during spin-coating on homogeneous substrates is based on the thermodynamic theories of polymer mixing and difference in solubility parameters of the two polymers

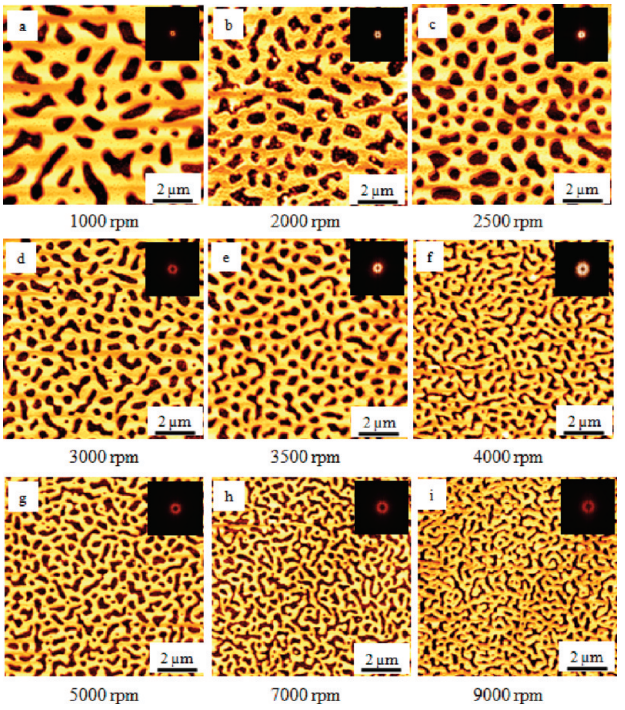

Figure 1. AFM topography images of phase-separated morphologies of PS/PAA blends on homogeneous substrates with a single surface energy. The scanning size was 10 μm × 10 μm. The spin speed was varied: (a) 1000, (b) 2000, (c) 2500, (d) 3000, (e) 3500, (f) 4000, (g) 5000, (h) 7000, and (i) 9000 rpm. Corresponding FFT diagram for each AFM image was inserted.

in their common solvent.[45,49] Fast Fourier transform (FFT) analysis of each image is also shown in Figure 1. The domain size of the morphologies decreased with increasing spin speed. Round diffusion rings were observed in the FFT analysis, indicating that the initial morphologies are isotropic.[50]

The diameter of the diffusion ring (i.e., the wave vector at which the intensity of the FFT diffusion ring is maximum), k^*, can be used to calculate the characteristic length, $1/k^*$.[30,51] With increasing spin speed, the diameters of the diffusion rings increased (Figure 1). Figure 2 shows the relationship between spin speed and characteristic length of PS/PAA phase-separated morphologies. With increasing spin speed, the characteristic length decreased. Phase separation and domain coarsening behaviors of PS/PAA blend during spin-coating are time dependent. Because the evaporation of the mutual solvent (DMF) was accelerated with increasing spin speed, the time available for the phase separation and domain coarsening of the PS/PAA blend was reduced. These kinetically driven behaviors resulted in a reduction of the characteristic length of the PS/PAA blend. Raczkowaska et al.[30] reported the relationship between characteristic length and processing conditions as $R = c/\omega^{1/2}$. We generalized this equation as

$$R = k\omega^{\alpha}c^{\beta} \quad (1)$$

where R denotes the characteristic length, k is the constant, and ω and c are spin speed and solution concentration, respectively. When the results in Figure 2 were fit to eq 1, the exponent for spin speed, α, was −0.71. The k and c were 3×10^5 nm/(rpm$^{-0.71}$ × wt %) and 1.0 wt %. Similar results were also found by Walheim et al.[45] for the effect of spin speed on the domain size of a PS/PMMA blend. By increasing spin speed, the domain size of the phase-separated morphology of a PS/PMMA blend could be reduced. Increased spin speed

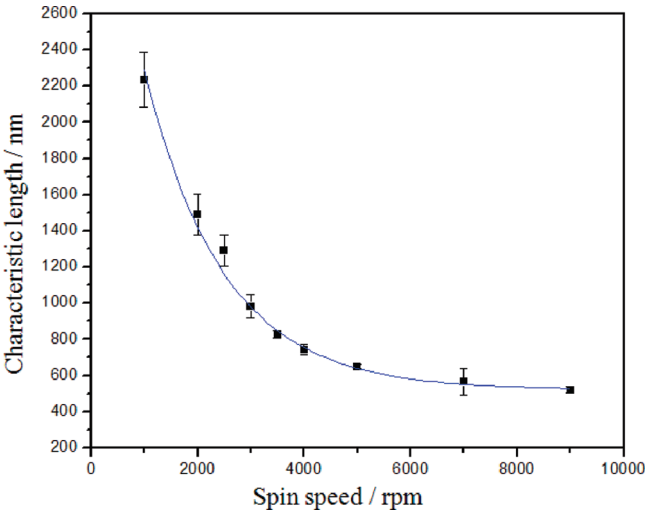

Figure 2. Effect of spin speed on the characteristic lengths of PS/PAA phase-separated morphologies.

also decreases film thickness, leading to smaller domain sizes with the rapid evaporation of solvent.

Heterogeneous Patterns with Constant Periodicity. The effect of spin speed on the directed assembly of PS/PAA blend on the heterogeneous patterns with constant periodicity was then studied. Figure 3 shows the FESEM images of the PS/PAA polymer blend solution spin-coated at different spin speeds on the alternating MUAM/ODT patterns with a constant periodicity of 1000 nm. The phase separation and domain coarsening of PS/PAA blends generated two distinct phases, with dark areas being attributed to PS and the light regions to PAA (Figure 3).[37] Similar to the driving force on homogeneous substrates, the thermodynamic driving force for phase separation also occurs with heterogeneous patterned substrates. In the case of heterogeneous substrates, however, the phase domains selectively wet their chemically attractive patterns and dewet the chemically unfavorable surfaces, driven by the polymer−surface interactions.[34] According to the requirement for commensurability between characteristic length and pattern periodicity for the perfect directed assembly,[30] we expected that well-ordered patterned structures of PS/PAA blend would occur when the characteristic length was close to the pattern periodicity of 1000 nm. The critical spin speed to produce the required characteristic length of 1000 nm was calculated to be 3082 rpm using eq 1.

Figure 3d shows the directed morphologies of PS/PAA blend at spin speeds of 3000 rpm. Because the spin speeds were close to the critical value of 3082 rpm, the resultant characteristic lengths were similar to the required characteristic length for the given pattern periodicity of 1000 nm. Therefore, good pattern replication was achieved. When the spin speeds were slower than 3000 rpm (Figure 3a−c), poor replication of the patterns was observed because the characteristic lengths were larger than the given pattern periodicity of 1000 nm. Figure 3e−i shows the patterned PS/PAA structures at spin speeds higher than 3000 rpm. As the spin speed increased, the characteristic lengths became increasingly smaller compared to the pattern periodicity of 1000 nm. Poor pattern replication was observed. With increasing spin speed, more PAA domains were trapped in PS domains as shown in Figure 3e−i. In order to fabricate well-ordered morphologies on patterns with constant periodicity, spin speed can be controlled to produce the required characteristic length to be commensurate with the given pattern periodicity. The fabrication of well-ordered directed morphologies of polymer

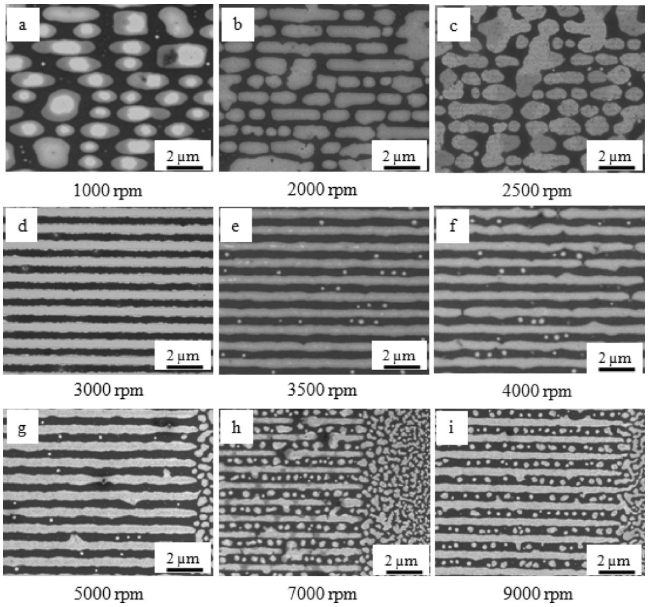

Figure 3. FESEM images of the directed PS/PAA morphologies on alternative MUAM/ODT patterns with 1000 nm periodicity. The dark regions are PS domains and the gray regions are attributed to PAA domains. The spin speeds were varied: (a) 1000, (b) 2000, (c) 2500, (d) 3000, (e) 3500, (f) 4000, (g) 5000, (h) 7000, and (i) 9000 rpm.

blends has been reported to require geometric commensuration between the characteristic length and pattern periodicity.[30] When the characteristic length is greater than the pattern periodicity, the larger domains completely wet the chemically more attractive surface (pattern), but excess material spills over onto more energetically unfavorable surfaces of the pattern. For characteristic lengths smaller than the pattern periodicity, there may be insufficient material to completely wet the energetically favorable surfaces, forming discontinuous patterns.

Heterogeneous Patterns with Different Periodicities. Well-ordered replication of patterns occurred when the given pattern periodicity was commensurate with the characteristic length, which can be controlled by spin speed. The effect of spin speed on replication of patterns with different periodicities (333−1333 nm) was investigated. Figure 4 shows the FESEM images of directed morphologies of the PS/PAA blend on MUAM/ODT patterns with different periodicities. The replication of patterns with 1333 nm periodicity at different spin speeds are shown in Figure 4a−d. For good directed assembly, the characteristic length should be equal to the pattern periodicity of 1333 nm. On the basis of eq 1, the critical spin speed to fabricate the required characteristic length of 1333 nm was calculated to be 2056 rpm. Because all the spin speeds used (3000−9000 rpm) were faster than the critical spin speed of 2056 rpm, the resultant characteristic lengths were smaller than 1333 nm and poor replication of the patterns was observed. Figure 4e−h presents the effect of spin speed on the directed assembly on patterns with a 1000 nm periodicity. As shown in Figure 4e, well-ordered patterned structures of the PS/PAA blend were produced because the spin speed of 3000 rpm was close to the calculated critical spin speed of 3082 rpm. Increasing the spin speed resulted in smaller characteristic lengths compared to the pattern periodicity of 1000 nm and resulted in increasingly disordered patterned morphologies (Figure 4f−h). Figure 4i−l shows the directed assembly on patterns of 667 nm periodicity. The critical spin speed to obtain the required characteristic length of 667 nm was calculated to be 5452 rpm.

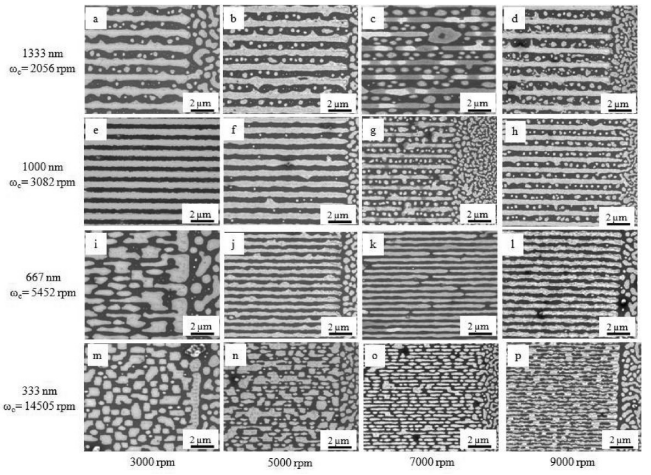

Figure 4. FESEM images of directed assembly of PS/PAA blends using alternative MUAM/ODT patterns with various periodicities: (a−d) 1333, (e−h) 1000, (i−l) 667, and (m−p) 333 nm. The spin speeds were changed: (a, e, i, m) 3000, (b, f, j, n) 5000, (c, g, k, o) 7000, and (d, h, l, p) 9000 rpm. ω_c stands for the critical spin speed for each pattern periodicity.

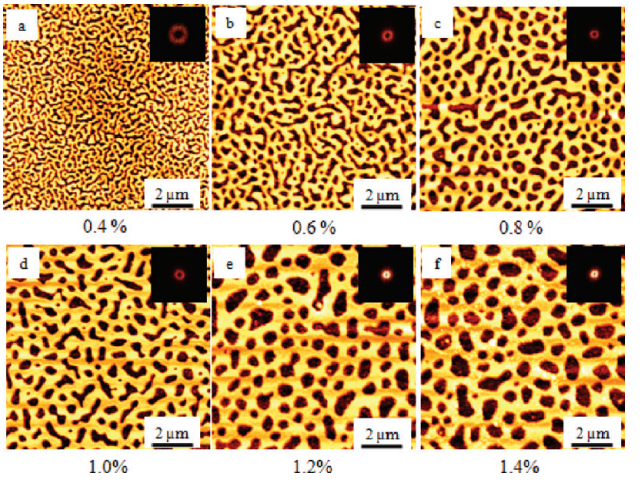

Figure 5. AFM topography images of PS/PAA blends films on homogeneous substrate with a single surface energy. The scanning size was 10 μm × 10 μm. The solution concentration was varied: (a) 0.4, (b) 0.6, (c) 0.8, (d) 1.0, (e) 1.2, and (f) 1.4 wt %. Corresponding FFT diagram for each AFM image was inserted.

When spin speeds were either lower or higher than the critical spin speed, poor assembly was observed. Spin speeds of 5000 and 7000 rpm produced characteristic lengths of 643 and 565 nm, respectively, and good directed assembly (Figure 4j,k). Figure 4m−p shows the morphologies for a pattern with a 333 nm periodicity. The corresponding critical spin speed to obtain a commensurate characteristic length was 14505 rpm. Because the spin speeds used were lower than the critical value, poor assembly occurred.

These results show that control of the spin speed can be used to obtain the required characteristic length commensurate with the pattern periodicity. Spin speed controls phase separation and domain coarsening. The pattern-directed dewetting/wetting behaviors of PS/PAA blend are also time-dependent. As the solvent evaporates, the polymer mobility is reduced; eventually patterning ceases. The evaporation rate of the solvent is increased with increasing spin speed, reducing the time available for directed assembly. Solution concentration also affects polymer mobility and time available for assembly and can be used to achieve the good assembly on patterns when the spin speed is experimentally inaccessible.

Solution Concentration. Solution concentration can also control the characteristic length. The effect of solution concentration on the characteristic length was investigated on homogeneous surfaces and heterogeneous patterns.

Homogeneous Substrates. To investigate the relationship between solution concentration and the characteristic length of a PS/PAA blend, solutions with different concentrations were spin-coated on homogeneous substrates. Figure 5 shows the phase-separated morphologies as measured using AFM and FFT. The domain size decreased with more dilute solutions. The round diffusion rings in the corresponding FFT diagrams indicate that the morphology was isotropic on the homogeneous substrate. The influence of solution concentration on the characteristic length of the PS/PAA blend is shown in Figure 6. The characteristic length increased linearly as the solution concentration was increased from 0.4 to 1.4 wt %. During spin-coating, the polymer blend solution spreads uniformly on the substrate, forming a liquid film. The spreading of this film is controlled by competition between centrifugal and viscous forces. With increasing solution concentration, the viscous forces increase, restricting film thinning. A thicker film provides a longer period of time for the

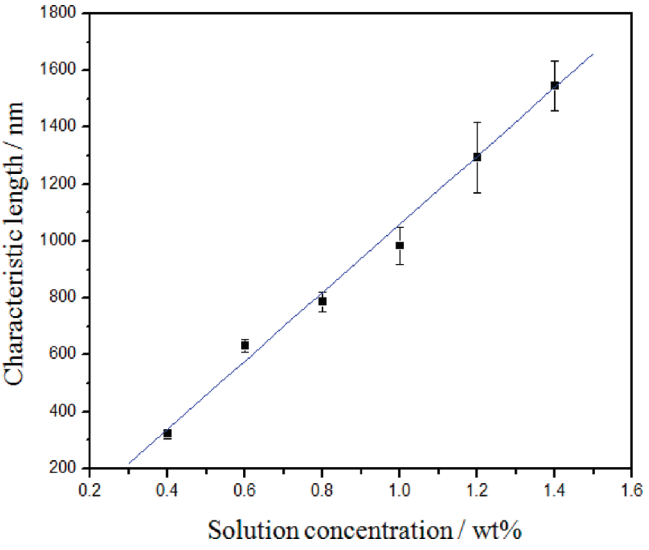

Figure 6. Relationship between solution concentration and the characteristic lengths of PS/PAA phase-separated morphologies.

solvent to evaporate and for phase separation and domain coarsening, resulting in an increased characteristic length. For PS/PVP blends, Raczkowska et al.[30] found that the characteristic length increased linearly with increasing solution concentration. Ton-That et al.[47] also found that the domain sizes of PS/PMMA blends were increased linearly by increasing solution concentration and that solution concentration could be used to control the domain size of polymer blends. Similarly, the domain height difference between PS and PAA decreased with reducing solution concentration because a shorter period of time was available for domain coarsening.

Heterogeneous Patterns with Constant Periodicity. The influence of solution concentration on the directed assembly for patterns with 1000 nm periodicity is shown in Figure 7. Since directed assembly is best when the characteristic length is commensurate with the pattern periodicity, well-ordered patterning was expected for a solution concentration producing a characteristic length of 1000 nm. Using the relationship between characteristic length and solution concentration (Figure 6), the critical solution concentration was calculated to be 0.96 wt %.

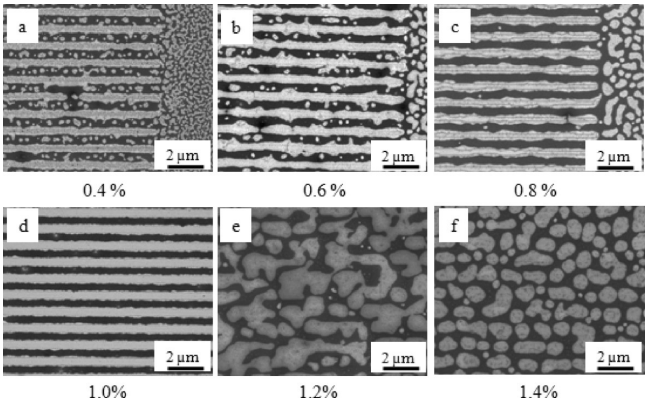

Figure 7. FESEM images of the directed PS/PAA morphologies on the MUAM/ODT alternative patterns with 1000 nm periodicity. The dark regions are PS domains and the gray regions are attributed to PAA domains. When the spin speed remained constant as 3000 rpm, solution concentrations were varied: (a) 0.4, (b) 0.6, (c) 0.8, (d) 1.0, (e) 1.2, and (f) 1.4 wt %.

As shown in Figure 7, the directed assembly on patterns with constant periodicity varied with solution concentration. For solution concentrations smaller than 0.96 wt % (Figure 7a−c), the characteristic lengths were smaller than the pattern periodicity and disordered patterned structures were observed. Figure 7d shows the morphology when the solution concentration was close to the critical value of 0.96 wt %. In this case, good assembly was observed. As shown in Figure 7e,f, increasing the solution concentration to 1.2 and 1.4 wt % produced characteristic lengths that were larger than the pattern periodicity, and the morphology became disordered again. By controlling solution concentration, Raczkowska et al.[30] and Walheim et al.[45] also found that well-ordered morphologies were produced when the produced characteristic length was commensurate with the pattern periodicity for blends of PS/PVP and PS/partially brominated polystyrene (PSBr), respectively. The use of spin speed and solution concentration together to control the characteristic ratio to achieve well-ordered pattern replication on the nanoscale, as well as the required level of commensurability, was not investigated in these studies.[30,45]

Heterogeneous Pattern with Different Periodicities. For the fabrication of well-ordered morphologies on patterns with different periodicities, control of the solution concentration is important. Solution concentration can be varied to produce the required characteristic length commensurate with the corresponding pattern periodicity.

Figure 8 shows the FESEM images of the directed assembly of the PS/PAA blend on patterns with different periodicities. For a pattern periodicity of 1333 nm (Figure 8a−d), the required solution concentration was calculated to be 1.24 wt %. All the solutions concentrations were smaller than 1.24 wt %, so the resulting characteristic lengths were smaller than the pattern periodicity and disordered morphologies were observed. When the pattern periodicity was reduced to 1000 nm (Figure 8e−h), a solution concentration of 0.96 wt % was required to obtain the commensurate characteristic length and well-ordered assembly (see Figure 8e). For a pattern periodicity of 667 nm, the critical solution concentration was calculated to be 0.68 wt % between the experimental concentrations of 0.6 (Figure 8j) and 0.8 wt % (Figure 8k). For these concentrations, good patterning was observed, while for concentrations smaller (0.4 wt %, Figure 8i) or larger (1.0 wt %, Figure 8l) poor assembly was produced. Figure 8m−p presents the morphologies on patterns with 333 nm periodicity. Figure 8p shows the well-ordered assembly produced

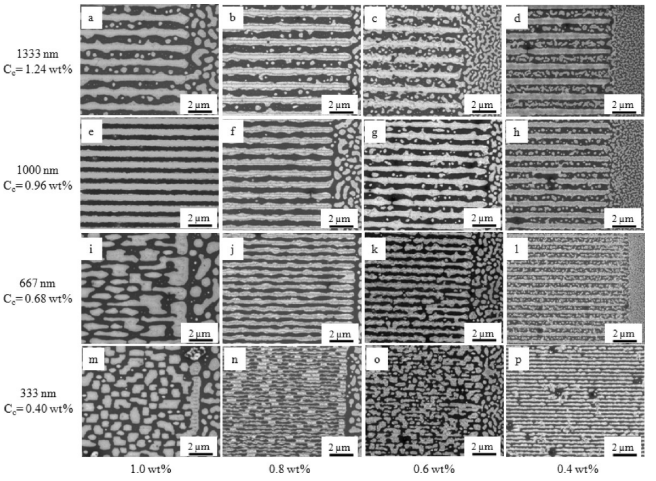

Figure 8. FESEM images of directed assembly of PS/PAA blends using alternative MUAM/ODT patterns with various periodicities: (a−d) 1333, (e−h) 1000, (i−l) 667, and (m−p) 333 nm. The solution concentrations were changed: (a, e, i, m) 1.0, (b, f, j, n) 0.8, (c, g, k, o) 0.6, and (d, h, l, p) 0.4 wt %. C_c stands for the critical solution concentration for each pattern periodicity.

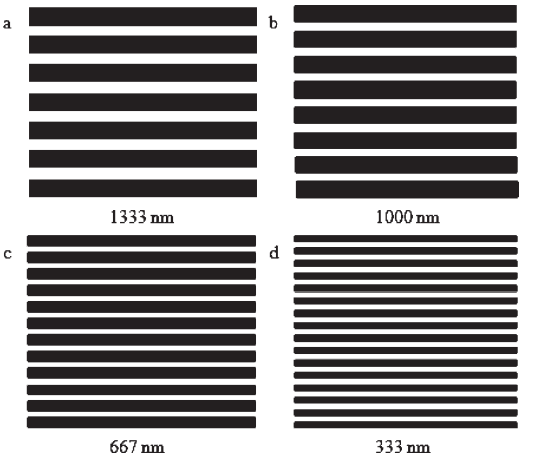

Figure 9. Schematic diagrams of the predesigned patterns with different periodicities: (a) 1333, (b) 1000, (c) 667, and (d) 333 nm.

when the solution concentration matched the critical solution concentration of 0.4 wt %. For solution concentrations larger than 0.4 wt %, (Figure 8m−o), disordered patterned morphologies were observed. Although for a concentration of 0.4 wt % the characteristic length was close to the pattern periodicity of 333 nm, some defects were still observed, indicating kinetic factors may still play a role. Similar to spin speed, solution concentration can also be controlled to produce characteristic length commensurate with the pattern periodicity to achieve excellent directed assembly of a PS/PAA blend.

Quantification. To quantitatively measure the directed assembly of a PS/PAA blend, a new method of image analysis was developed. In this method, the actual patterned morphologies seen in the FESEM images were compared with the corresponding pattern geometries, considered to be perfect assembly (Figure 9). Patterning efficiency, E_p, a dimensionless parameter, was introduced to quantify the relationship between the template and the assembled polymer blend, as shown in the equation

$$E_p = 1 - \frac{\sum_{i=1}^{N} |S_i - S_{0,i}|}{2N} \quad (2)$$

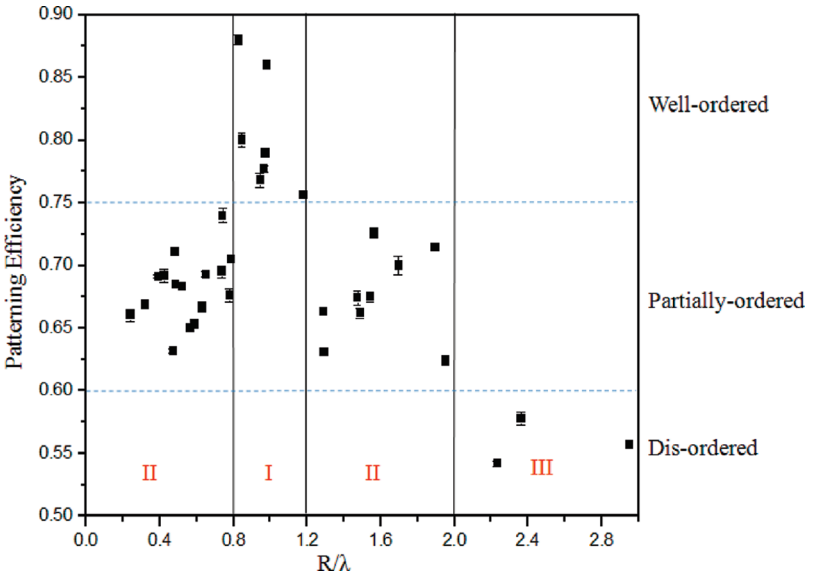

Figure 10. Relationship between the patterning efficiency and the ratio of R/λ.

where N is the number of the pixels. $S_{0,i}$ is attributed to the grayscale of the corresponding pixel i in the predesigned patterns. $S_{0,i}$ equals 1 when the dark regions are taken to be PS domains, and $S_{0,i}$ equals -1 when the bright areas in the predesigned patterns are taken to be PAA domains (Figure 9). S_i denotes the grayscale found in the FESEM images for pixel i. When the grayscale at pixel i was greater than 127, pixel i was considered a dark region and S_i is given a value of 1. When the grayscale at pixel i was smaller than 127, pixel i was considered as a white region and S_i is given a value of -1. The resultant values of E_p vary from 0.5 to 1. When E_p equals 0.5, the phase-separated morphologies are not affected by the chemically heterogeneous patterns and are isotropic. When E_p equals 1, perfect replication of the underlying pattern is produced. For each FESEM image, five different areas were randomly chosen and compared with their corresponding pattern geometries having the same size and pixel number. Five different patterning efficiencies were calculated and used to obtain the average and standard deviation (used for error bars).

For each FESEM image the patterning efficiency was measured and compared to the ratio of the characteristic length to the respective pattern periodicity, R/λ. Figure 10 shows the effect of R/λ on the patterning efficiency. Three levels of replication were defined in Figure 10. When $0.5 < E_p < 0.6$, the directed morphologies were considered disordered. Partially ordered and well-ordered patterned structures were defined when $0.6 < E_p < 0.75$ and $E_p > 0.75$, respectively. Values for $E_p > 0.75$ were found when $0.8 < R/\lambda < 1.2$ (region I). It is widely accepted that when the characteristic length is commensurate with the pattern periodicity, i.e., $R/\lambda = 1$, perfect directed morphologies are produced. Here it is seen that for well-ordered directed assembly of polymer blends the range of the commensurability should be within 20%. Values for $0.6 < E_p < 0.75$ were found when $R/\lambda < 0.8$ (values of $R/\lambda < 0.2$ were not investigated) or $1.2 < R/\lambda < 2.0$ (region II). In this region, partially ordered patterned structures were produced. Values for $E_p < 0.6$ were found when $R/\lambda > 2.0$ (region III). In this region, disordered (nearly isotropic) structures were produced.

Conclusions

Nanopatterned polymer structures can be produced by directed assembly of polymer blends on chemically heterogeneous patterns during spin-coating. Well-ordered polymer morphologies can be produced when the characteristic length of polymer blends, R, is commensurate with pattern periodicity, λ. Control of the characteristic length to be commensurate with pattern periodicity is important for the fabrication of well-ordered directed morphologies in polymer blends. In this paper, spin-coating speed and solution concentration were used to control the characteristic length of a PS/PAA blend and to produce the well-ordered morphologies.

The characteristic length was reduced by increasing spin speed from 1000 to 9000 rpm or reducing solution concentration from 1.4 to 0.4%. For the directed assembly on patterns with periodicity of 1000 nm, a well-ordered morphology was produced when spin speed was 3000 rpm and solution concentration was 1.0%. Under this condition, the characteristic length was commensurate with the pattern periodicity. For the replication of patterns with different periodicities (333−1333 nm), the critical spin speeds or solution concentrations, producing the required characteristic lengths to be commensurate with the given pattern periodicities, were predicted. Well-ordered morphologies were found when the spin speed or solution concentration was close to the critical value. Disordered morphologies were observed when the spin speed or solution concentration was larger or smaller than the critical value.

In this paper, the range of commensurability between characteristic length and pattern periodicity for well-ordered morphologies of polymer blends was discussed for the first time. A new method was introduced to quantitatively evaluate the directed morphologies based on image analysis. It was observed that when R and λ were within 20% of each other ($0.8 < R/\lambda < 1.2$), well-ordered morphologies were produced. When $R/\lambda < 0.8$ or $1.2 < R/\lambda < 2.0$, partially ordered morphologies were found. Disordered morphologies occurred when $R/\lambda > 2.0$.

In this paper, the effect of processing parameters, such as spin speed and concentration, on the fabrication of nanoscale patterned polymer blends is reported. This work is important for the development of high rate nanomanufacturing methods to accelerate the commercialization of nanostructured polymers for a variety of applications.

Acknowledgment. The authors thank the support of the National Science Foundation (Award # NSF-0425826). We also appreciate the Kostas Center for the preparation of templates.

References and Notes

(1) Guarini, K. W.; Black, C. T.; Zhang, Y.; Babich, I. V.; Sikorski, E. M.; Gignac, L. M. *IEEE Int. Electron Devices Meet., Tech. Dig.* **2003**, 541.
(2) Park, M.; Harrison, C.; Chaikin, P. M.; Register, R. A.; Adamson, D. H. *Science* **1997**, *276*, 1401.
(3) Li, R. R.; Dapkus, P. D.; Thompson, M. E.; Jeong, W. G.; Harrison, C.; Chaikin, P. M.; Register, R. A.; Adamson, D. H. *Appl. Phys. Lett.* **2000**, *76*, 1689.
(4) McClelland, G. M.; Hart, M. W.; Rettner, C. T.; Best, M. E.; Carter, K. R.; Terris, B. D. *Appl. Phys. Lett.* **2002**, *81*, 1483.
(5) Cheng, J. Y.; Ross, C. A.; Thomas, E. L.; Smith, H. I.; Vancso, G. J. *Appl. Phys. Lett.* **2002**, *81*, 3657.
(6) Maury, P.; Escalante, M.; Reinhoudt, D. N.; Huskens, J. *Adv. Mater.* **2005**, *17*, 2718.
(7) Kim, Y. S.; Lee, N. Y.; Lim, J. R.; Lee, M. J.; Park, S. *Chem. Mater.* **2005**, *17*, 5867.
(8) Yin, Y.; Xia, Y. *J. Am. Chem. Soc.* **2003**, *125*, 2048.
(9) Yang, C. H.; Shin, T. J.; Yang, L.; Cho, K.; Ryu, C. Y.; Bao, Z. N. *Adv. Funct. Mater.* **2005**, *15*, 671.
(10) Stingelin-Stuntzmann, N.; Smits, E.; Wondergem, H.; Tanase, C.; Blom, P.; Smith, P.; Leeuw, D. D. *Nature Mater.* **2005**, *4*, 601.
(11) Kline, R. J.; McGehee, M. D.; Toney, M. F. *Nature Mater.* **2006**, *5*, 328.
(12) Morteani, A. C.; Sreearunothai, P.; Herz, L. M.; Friend, R. H.; Silva, C. *Phys. Rev. Lett.* **2004**, *92*, 247402.
(13) Morteani, A. C.; Dhoot, A. S.; Kim, J. S.; Silva, C.; Greenham, N. C.; Murphy, C.; Moons, E.; Cina, S.; Burroughes, J. H.; Friend, R. H. *Adv. Mater.* **2003**, *15*, 1708.
(14) Wenzl, F. P.; Pachler, P.; Suess, C.; Haase, A.; List, E. J. W.; Poelt, P.; Somitsch, D.; Knoll, P.; Scherf, U.; Leising, G. *Adv. Funct. Mater.* **2004**, *14*, 441.
(15) Edwards, E. W.; Stoykovich, M. P.; Nealey, P. F. *J. Vac. Sci. Technol., B* **2006**, *24*, 340.
(16) Craig, G. S. W.; Nealey, P. F. *J. Photopolym. Sci. Technol.* **2007**, *20*, 511.
(17) Craig, G. S. W.; Nealey, P. F. *J. Vac. Sci. Technol., B* **2007**, *25*, 1969.
(18) Stoykovich, M. P.; Edwards, E. W.; Solak, H. H.; Nealey, P. F. *Phys. Rev. Lett.* **2006**, *97*, 147802.
(19) Stoykovich, M. P.; Kang, H.; Daoulas, K. Ch.; Liu, G. L.; Liu, C.-C.; de Pablo, J. J.; Muller, M.; Nealey, P. F. *ACS Nano* **2007**, *1*, 168.
(20) Kim, S. O.; Solak, H. H.; Stoykovich, M. P.; Ferrier, N. J.; de Pablo, J. J.; Nealey, P. F. *Nature* **2003**, *424*, 411.
(21) Park, S. M.; Ravindran, P.; La, Y. H.; Craig, G. S. W.; Ferrier, N. J.; Nealey, P. F. *Langmuir* **2007**, *23*, 9037.
(22) Yang, X. M.; Peters, R. D.; Nealey, P. F. *Macromolecules* **2000**, *33*, 9575.
(23) La, Y. H.; Stoykovich, M. P.; Park, S. M.; Nealey, P. F. *Chem. Mater.* **2007**, *19*, 4538.
(24) Schaffer, E.; Thurn-Albrecht, T.; Russell, T. P.; Steiner, U. *Nature* **2000**, *403*, 874.
(25) Rockford, L.; Liu, Y.; Mansky, P.; Russell, T. P. *Phys. Rev. Lett.* **1999**, *82*, 2602.
(26) Rockford, L.; Mochrie, S. G. J.; Russell, T. P. *Macromolecules* **2001**, *34*, 1487.
(27) Thurn-Albrecht, T.; DeRouchy, J.; Russell, T. P.; Jaeger, H. M. *Macromolecules* **2000**, *33*, 3250.
(28) Stoykovich, M. P.; Muller, M.; Kim, S. O.; Solak, H. H.; Edwards, E. W.; de Pablo, J. J.; Nealey, P. F. *Science* **2005**, *308*, 1442.
(29) Bergues, B.; Lekki., J.; Budkowski, A.; Cyganik, P.; Lekka, M.; Bernasik, A.; Rysz, J.; Postawa, Z. *Vacuum* **2001**, *63*, 297.
(30) Raczkowska, J.; Cyganik, P.; Budkowski, A.; Bernasik, A.; Rysz, J.; Raptis, I.; Czuba, P.; Kowalkski, K. *Macromolecules* **2005**, *38*, 8486.
(31) Raczkowska, J.; Bernasik, A.; Budkowski, A.; Cyganik, P.; Rysz, J.; Raptis, I.; Czuba, P. *Surf. Sci.* **2006**, *600*, 1004.
(32) Cyganik, P.; Bernasik, A.; Budkowski, A.; Bergues, B.; Kowalski, K.; Rysz, J.; Lekki, J.; Lekka, M.; Postawa, Z. *Vacuum* **2001**, *63*, 307.
(33) Coffey, D. C.; Ginger, D. S. *J. Am. Chem. Soc.* **2004**, *127*, 4564.
(34) Wei, J. H.; Coffey, D. C.; Ginger, D. S. *J. Phys. Chem. B* **2006**, *110*, 24324.
(35) Karim, A.; Douglas, J. F.; Lee, B. P.; Glotzer, S. C.; Rogers, J. A.; Jackman, R. J.; Amis, E. J.; Whitesides, G. M. *Phys. Rev. E* **1998**, *57*, R6273.
(36) Ermi, B. D.; Nisato, G.; Douglas, J. F.; Rogers, J. A.; Karim, A. *Phys. Rev. Lett.* **1998**, *81*, 3900.
(37) Wei, M.; Fang, L.; Lee, J.; Somu, S.; Xiong, X. G.; Barry, C.; Busnaina, A.; Mead, J. *Adv. Mater.* **2009**, *21*, 794.
(38) Böltau, M.; Walheim, S.; Mlynek, J.; Krausch, G.; Steiner, U. *Nature* **1998**, *391*, 877.
(39) Chiota, J.; Shearer, J.; Wei, M.; Barry, C.; Mead, J. *Small* **2009**, *5*, 2788.
(40) Xia, H. Sh.; Song, M. *Thermochim. Acta* **2005**, *429*, 1.
(41) Yan, L. T.; Sheng, J. *Polymer* **2006**, *47*, 2894.
(42) Ma, G. Q.; Zhao, Y. H.; Yan, L. T.; Li, Y. Y.; Sheng, J. *J. Appl. Polym. Sci.* **2006**, *100*, 4900.
(43) Han, X.; Liu, H. L.; Hu, Y. *J. Polym. Sci., Part B: Polym. Phys.* **2007**, *45*, 532.
(44) Wang, P.; Koberstein, J. T. *Macromolecules* **2004**, *37*, 5671.
(45) Walheim, S.; Böltau, M.; Mlynek, J.; Krausch, G.; Steiner, U. *Macromolecules* **1997**, *30*, 4995.
(46) Cui, L.; Ding, Y.; Li, X.; Wang, Zh.; Han, Y. Ch. *Thin Solid Films* **2006**, *515*, 2038.
(47) Ton-That, C.; Shard, A. G.; Bradley, R. H. *Polymer* **2002**, *43*, 4973.
(48) Nisato, G.; Ermi, B. D.; Douglas, J. F.; Karim, A. *Macromolecules* **1999**, *32*, 2356.
(49) Heriot, S.; Jones, R. *Nature Mater.* **2005**, *4*, 782.
(50) Fang, L.; Wei, M.; Shang, Y. R.; Jimenez, L.; Kazmer, D.; Barry, C.; Mead, J. *Polymer* **2009**, *50*, 5837.
(51) Kim, Y. H.; Okamoto, M.; Kotaka, T. *Macromolecules* **2000**, *33*, 8113.